

# Orbital Ordering in Paramagnetic $\text{LaMnO}_3$ and $\text{KCuF}_3$ .

J. E. Medvedeva<sup>1,2</sup>, M. A. Korotin<sup>1</sup>, V. I. Anisimov<sup>1</sup>, A. J. Freeman<sup>2</sup>

<sup>1</sup> *Institute of Metal Physics, Yekaterinburg, Russia.*

<sup>2</sup> *Department of Physics and Astronomy, Northwestern University, Evanston, Illinois*

*60208-3112.*

## Abstract

*Ab-initio* studies of the stability of orbital ordering, its coupling to magnetic structure and its possible origins (electron-phonon and/or electron-electron interactions) are reported for two perovskite systems,  $\text{LaMnO}_3$  and  $\text{KCuF}_3$ . We present a new Average Spin State (ASS) calculational scheme that allowed us to treat a paramagnetic state. Using this scheme, we successfully described the experimental magnetic/orbital phase diagram of both  $\text{LaMnO}_3$  and  $\text{KCuF}_3$  in crystal structures when the Jahn-Teller distortions are neglected. Hence, we conclude that the orbital ordering in both compounds is purely electronic in origin.

It is known from the earlier studies<sup>1,2</sup> that the magnetic order is coupled to the orbital one – magnetic interactions depend on the type of occupied orbitals of transition-metal ions. (A very detailed overview on magnetic and orbital ordering in cuprates and manganites was given recently by Oleś *et al*<sup>3</sup>.) For example, the orbital ordering in  $\text{LaMnO}_3$  reduces the ferromagnetic contribution from the  $e_g$  orbitals to the interlayer exchange coupling and is responsible for the stability of the magnetic ground state structure (which is A-type antiferromagnetic below  $T_N=141$  K<sup>4</sup>) — as described both experimentally and theoretically on this manganite<sup>1,4,5</sup>. Orbital ordering in  $\text{KCuF}_3$  was obtained in Kugel-Khomskii spin-orbital model<sup>2</sup> as a result of an exchange interaction which correctly describes both orbital and spin alignments simultaneously, so the spin and orbital degrees of freedom are mutually

coupled.

A more complicated picture of the fundamental connection between orbital ordering (OO) phenomena and forms of the spin alignments follows from experimental measurements that characterize an orbital order parameter and magnetic interactions in transition-metal oxides. Using the dipole resonant x-ray scattering technique, Murakami *et al.*<sup>6</sup> found a sharp disappearance of orbital ordering at much higher temperature ( $\sim 780$  K) than  $T_N$  in  $\text{LaMnO}_3$ . They suggested a coupling of the spin and orbital degrees of freedom due to the small decrease of the order parameter of the orbital structure above  $T_N$ , even despite the presence of orbital ordering in the paramagnetic phase of  $\text{LaMnO}_3$ . The most striking result was obtained for bilayered manganite,  $\text{LaSr}_2\text{Mn}_2\text{O}_7$ <sup>7</sup>: namely, a competition between the (charge-disordered) A-type AFM spin ordering with  $T_N \approx 170$  K and the CE-type<sup>4</sup> charge/orbital ordering (COO), which exists between  $T_N$  and COO transition temperature,  $T_{COO}=210$  K. With decreasing temperature the development of the charge/orbital ordering phase is disrupted by the onset of the A-type AFM ordering at  $T_N$ .

In this paper, we investigate the stability of observed orbital orderings without appealing to magnetic interactions by modeling the paramagnetic phase of two manganites,  $\text{LaMnO}_3$  and  $\text{KCuF}_3$ . To this end, we examined all magnetic configurations that are mathematically possible in the unit cell of the perovskites which consists from 4 Mn (or Cu) atoms. There are only eight such spin sets – as schematically presented in Fig. 1. They include the possibility of having ferromagnetic (labelled "1"), C-type ("3"), A-type ("6") and G-type ("7") antiferromagnetic spin orderings – as well as four configurations that do not have a physical meaning, i.e., cannot be realized as an individual magnetically ordered solution. Then, to model a paramagnetic state, during the iterations towards a self-consistency, we average the orbital occupation matrices (that contain information on the orbital polarization and orbital ordering in the unit cell) and potential parameters of all atoms over eight spin alignment configurations after each iteration. As a result, we have an averaged spin state (ASS) and can analyze the stability/presence of orbital polarization in such a modeled paramagnetic phase. Self-consistency of the ASS calculation is determined by convergence

of the averaged total energy, charge densities and orbital occupation matrices.

Typically, the origin of the orbital polarization is believed to be the electron-phonon interaction (the Jahn-Teller distortion) and the electron-electron interaction. A cooperative Jahn-Teller (JT) effect which sets in well above the magnetic transition temperature, stabilizes the particular order of the partly filled  $e_g$  orbitals that are close to orbital degeneracy<sup>8</sup>. Monte Carlo investigations<sup>9</sup> showed a stabilization of the experimental magnetic and orbital orderings in  $\text{LaMnO}_3$  only after including lattice distortions. However, a spin-orbital model for insulating undoped  $\text{LaMnO}_3$  derived in<sup>10</sup> explains (although qualitatively) the observed A-type antiferromagnetism as stabilized by a purely electronic mechanism.

We investigated two typical pseudocubic perovskites: *(i)*  $\text{LaMnO}_3$ , in which the strong cooperative Jahn-Teller effect breaks the degeneracy of the electronic configuration of  $\text{Mn}^{3+}$  ( $t_{2g}^3 e_g^1$ ) and directly affects the  $e_g$  orbital population. A recent high-resolution neutron-powder diffraction study, together with thermal analysis<sup>11</sup>, showed that  $\text{LaMnO}_3$  undergoes a structural phase transition at  $T_{JT}=750$  K above which the orbital ordering disappears. To establish the origin of orbital ordering in  $\text{LaMnO}_3$ , we performed ASS calculations for the high temperature crystal structure where cooperative Jahn-Teller distortions are absent. The experimental diffraction data<sup>11,12</sup> can be interpreted using two crystal symmetries – double-cubic orthorhombic  $Pbnm$  structure and rhombohedral  $R\bar{3}c$  crystal structure – and we did calculations for both of them. *(ii)* Another example of a perovskite compound with partly occupied  $e_g$  orbitals resulting in strong Jahn-Teller distortions and strong one-dimensional antiferromagnetic interactions is  $\text{KCuF}_3$ . Experimental studies showed that there are two tetragonal crystal types of  $\text{KCuF}_3$ <sup>13,14</sup>, which are stable in a wide temperature range, and their A-type antiferromagnetic ordering temperatures are equal to 20 K and 38 K. It was shown<sup>15</sup> for this compound that the ground state with the lattice distortion and the orbital polarization (and ordering) can be stabilized only by taking into account the Coulomb correlation between d-shell electrons (LDA+U approach). We performed ASS calculations for a model structure of  $\text{KCuF}_3$  in which the experimentaly observed Jahn-Teller distortions were not included.

In order to address the orbital ordering observed in manganites, it is necessary to go beyond the local (spin) density approximation (L(S)DA) by including the intra d-shell Coulomb interaction (LDA+U method<sup>16</sup>). In our calculations we use U=8 eV and J=0.88 eV as those relevant to the actual manganese oxides parameters<sup>16–18</sup>.

*LaMnO<sub>3</sub>*. As the first step, we performed LSDA+U calculations for the experimental A-type antiferromagnetic phase of LaMnO<sub>3</sub> with low-temperature *Pbnm* structure (where strong cooperative Jahn-Teller distortions are present). The self-consistent non-diagonal occupation matrix for the spin density of the *e<sub>g</sub>* subshell ( $3z^2 - r^2$  and  $x^2 - y^2$  orbitals) of one particular Mn atom is found to be

$$n_{mm'}^{\uparrow} - n_{mm'}^{\downarrow} = \begin{pmatrix} 0.43 & 0.29 \\ 0.29 & 0.59 \end{pmatrix}.$$

The diagonalization of this matrix gives two new *e<sub>g</sub>* orbitals:  $\phi_1 = 3x^2 - r^2$  ( $3y^2 - r^2$  for the second type of Mn atom) with an occupancy of 0.81 and  $\phi_2 = z^2 - y^2$  ( $z^2 - x^2$ ) with an occupancy of 0.20. Since a Mn<sup>3+</sup> ion has formally one electron in the partially filled *e<sub>g</sub>*<sup>↑</sup> subshell and the *t<sub>2g</sub>*<sup>↑</sup> subshell is totally filled, we presented the resulting orbital ordering by plotting the angular distribution of the *e<sub>g</sub>* spin density (Fig. 2):

$$\rho(\theta, \phi) = \sum_{mm'} (n_{mm'}^{\uparrow} - n_{mm'}^{\downarrow}) Y_m(\theta, \phi) Y_{m'}(\theta, \phi)$$

where the  $Y_m(\theta, \phi)$  are corresponding spherical harmonics.

The resulting picture of the orbital ordering in the A-type antiferromagnetic LaMnO<sub>3</sub> is in very good agreement with that given by Goodenough in 1955<sup>1</sup> and recently detected using resonant x-ray scattering techniques<sup>6</sup>. Based on this result, we can now move to the case of  $T > T_N$  to investigate the region of the magnetic/orbital phase diagram where, according to<sup>6</sup>, the orbital ordering exists in the paramagnetic phase. To this end, we performed the model ASS calculations described above for the high-temperature (at T=798 K) structure of LaMnO<sub>3</sub> with lattice parameters taken from<sup>11</sup>. The paramagnetic iterations were started from uniform distribution of *e<sub>g</sub>* electrons over the  $3z^2 - r^2$  and  $x^2 - y^2$  orbitals of all Mn atoms. In the insert to Fig. 3 we plot the "total energy" of the paramagnetic state of the

high-temperature structure of  $\text{LaMnO}_3$  (crosses) obtained by averaging the total energies of the eight possible magnetic configurations. This total energy curve becomes saturated after the  $\sim 20$ th iteration, hence, we may call this ASS result self-consistent.

In order to illustrate the stability of orbital order in the paramagnetic phase and to compare the orbital polarization with that calculated for the experimental A-type AFM phase, we present the orbital order as a difference between the occupancies of the  $\phi_1$  and  $\phi_2$  orbitals which diagonalize spin density matrix in the  $e_g$ -subshell. In Fig. 3, this difference is shown plotted against the number of paramagnetic iterations (crosses). We found that starting with equal  $3z^2 - r^2$  and  $x^2 - y^2$  orbital occupancies (and with diagonal occupation matrix), the value of the non-diagonal elements of the occupation matrix grows during the ASS calculation leading to a saturated orbital polarization of the right type (the same type as obtained for A-type AFM  $\text{LaMnO}_3$ , c.f., Fig. 2) around the tenth iteration (c.f., Fig. 3). We should note here, that the orbital ordering in the paramagnetic state is the only stable solution. Forcing different orbital polarizations (ferro-orbitally ordered, etc.) as a starting one for the paramagnetic calculation resulted in the type of orbital ordering obtained above by changing the corresponding (non-diagonal) orbital occupancy during the iterations towards self-consistency. The horizontal line in Fig. 3 stands for the difference between  $\phi_1$  and  $\phi_2$  orbital occupancies obtained from the usual spin-polarized self-consistent LDA+U calculation for the A-type AFM phase of  $\text{LaMnO}_3$  in the low-temperature  $Pbnm$  structure. Comparing the orbital polarizations of the paramagnetic and antiferromagnetic phases (Fig. 3), we conclude that the AFM-PM transition in  $\text{LaMnO}_3$  results in a slight decrease of the difference between the  $\phi_1$  and  $\phi_2$  orbital occupancies but does not suppress it. This finding agrees with the observed behavior of the orbital ordering parameter when the temperature increases ( $T > T_N$ )<sup>6</sup>.

We need to point out here one essential feature of the ASS calculation. Since we consider a spin state averaged over eight magnetic configurations and therefore an average occupation matrix of such a paramagnetic state, it is interesting to analyze the deviation of the orbital polarization in each of these configurations from the averaged value. As can be seen from

Fig. 4, where we plot the  $\phi_1$  and  $\phi_2$  orbital occupancy difference for each of the eight spin configurations after the first (broken line) and fiftieth (solid line) paramagnetic iteration, the deviations from the average value become smaller with iterations – they decrease from 36% to 12%, correspondingly. (Further increases of the iteration number do not suppress the deviations, so the illustrated curve for the 50th iteration stays the same.) The variations at the beginning of the ASS calculation and for the obtained result, c.f., Fig. 4, have a close analogy in oscillation behavior, i.e., the location of the  $e_g$  orbital occupancy difference stays higher (lower) with respect to the average value for the same particular magnetic configuration during the iterations. Hence, one can separate the eight magnetic configurations into three groups: lowest located against the average value (configurations 1 and 2), highest located (4 and 7) and those close to the average value (3,5,6 and 8).

We analyzed possible reasons for this separation by calculating the number of ferro- or antiferro-spin aligned magnetic neighbours for the first Mn atom (note, that the spin of this Mn atom does not change in all eight configurations, Fig. 1). First of all, we found that the behavior of the  $e_g$  orbital occupancy difference curves (Fig. 4) is determined by the nearest neighbors spin alignment. For both the 1st and 2nd magnetic configurations, all six nearest neighbours of the first Mn atom (which is spin-up) have the same spin direction, so ferromagnetic couplings with all nearest neighbours give the smallest  $\phi_1 - \phi_2$  value. By contrast, the biggest contributions were obtained from configurations 4 and 7, where we have six antiferromagnetic couplings between the first Mn atom and its nearest neighbors. The third group of configurations possess two ferro- and four antiferromagnetic couplings (these are the 3rd and 8th configurations), giving almost an exact average value  $\phi_1 - \phi_2$ , and four ferro- and two antiferromagnetic couplings (5 and 6), both lying below the average value. (Note here, that it would be enough to consider only four magnetic configurations: 1st (which corresponds to FM phase), 3rd (C-type AFM phase), 6th (A-type AFM) and 7th (G-type AFM). Averaging over these four configurations underestimates the value averaged over all eight configurations only by 0.7 and 0.1 % for the first and 50th paramagnetic iteration, respectively.) Thus, we can conclude, that the antiferromagnetic spin alignment

seems to be more preferable for orbital ordering than the ferromagnetic one; however, the decrease of the  $\phi_1 - \phi_2$  deviation against the average values (from 47 to 17 % for the first and 50th iteration, respectively) at the FM phase (1st configuration) support the importance of the ferromagnetic coupling in ASS calculation as well as the antiferromagnetic one.

Now let us discuss some peculiarities in the crystal structure of LaMnO<sub>3</sub> related to the Jahn-Teller distortions. As it was found by recent neutron-powder diffraction studying<sup>11</sup>, the Jahn-Teller transition in this perovskite compound occurs at T=750 K. If we define the degree of tetragonal distortion as

$$\delta_{JT} = (d_l - d_s)/(d_l + d_s)/2$$

where  $d_l$  and  $d_s$  denoting the long and short Mn-O bond distance correspondingly, then according to the structural data from Ref.<sup>11</sup>,  $\delta_{JT}$  changes with heating from  $\delta_{JT}=0.133$  for the room temperature *Pbmn* structure to  $\delta_{JT}=0.023$  for the crystal structure at 798 K (which is also orthorombic *Pbmn*, but described as "double-cubic" perovskite<sup>19</sup>). Above, we reported calculations for both of these structures, and basing on the obtained results we may conclude that strong lattice distortions do not influence the orbital order. However,  $\delta_{JT}$  is not zero in the high-temperature structure and we have slightly different Mn-O bond distances which breakes the cubic symmetry, so the Jahn-Teller effect still may play some role in orbital ordering. To check this possibility, we perform ASS calculation for the rhombohedral *R* $\bar{3}c$  structure. The lattice parameters were taken from<sup>20</sup>. All Mn-O distances are equal in this structure, so  $\delta_{JT}=0.000$ . For this case, the obtained difference between occupancies of the  $\phi_1$  and  $\phi_2$  orbitals diagonalizing spin density matrix against the number of paramagnetic iteration shown in Fig. 3 (curcles). This difference is smaller than obtained for two orthorombic structures, nevertheless, we conclude that the orbital ordering does not disapeare in regular MnO<sub>6</sub> octahedra, and hence JT-distortions are not the origin of the orbital ordering in LaMnO<sub>3</sub>.

*KCuF<sub>3</sub>*. We also investigated the orbital structure in paramagnetic phase of another perovskite compound with partly occupied *e<sub>g</sub>* orbitals, KCuF<sub>3</sub>, by applying ASS calculation

scheme. As it was shown by Kugel and Khomskii<sup>2</sup>,  $\text{KCuF}_3$  is an example of system in which the exchange interaction alone results in the correct orbital ordering. *Ab-initio* LDA+U investigations<sup>15</sup> confirmed the electronic origin of the ordering: the coupling to the lattice is not a driving force for the orbital (and magnetic) ordering, but the lattice follows the orbital state. Hence, we performed ASS calculations for a model structure of  $\text{KCuF}_3$  in which cooperative JT lattice distortions were neglected. We used the tetragonal ( $P4/mmm$ ) crystal structure with  $a=5.855$  Å,  $c=7.846$  Å and coordinates for K (0, 0.5, 0.45), Cu (0, 0, 0), F1 (0, 0, 0.45) and F2 (0.25, 0.25, 0). In this structure, the  $\text{CuF}_6$  octahedra are slightly compressed along the  $c$  axis: the distance from the Cu atom to the apical F1 atom  $d(\text{Cu}-\text{F1})=1.96$  Å, while in the  $ab$ -plane  $d(\text{Cu}-\text{F2})=2.07$  Å (without the quadrupolar deformation in the  $ab$  plane that is present in the experimental structure).

Since this perovskite compound possesses two equivalent (by energy) types of orbital orderings characterized by alternation of the  $d_{x^2-z^2}$  and  $d_{y^2-z^2}$  orbitals<sup>2,21</sup>, we performed four ASS calculations which were started with different  $e_g$ -electron distributions over Mn  $e_g$  orbitals: the orbital polarizations chosen corresponded to F-type ferro-orbital and A-, C- or G-type antiferro-orbital alternations of  $d_{x^2-z^2}/d_{y^2-z^2}$  orbitals (shown in the upper row of orbital structures in Fig. 5); the C- and G- orbital configurations were observed experimentally<sup>21</sup>. Since a  $\text{Cu}^{2+}$  ion ( $d^9$  configuration) has one hole in the  $e_g$  state, we represent the orbital structures by a  $2\times 2$   $e_g$ -orbital occupation matrix,  $n_{mm'}^{\uparrow} - n_{mm'}^{\downarrow}$ . As a start we used the following non-diagonal occupation matrix for the spin density of the  $e_g$  sublattice of one particular Cu atom:

$$n_{mm'}^{\uparrow} - n_{mm'}^{\downarrow} = \begin{pmatrix} 0.53 & \pm 0.28 \\ \pm 0.28 & 0.15 \end{pmatrix},$$

the diagonalization of which gives  $d_{x^2-z^2}$  ( $d_{y^2-z^2}$ ) orbitals.

In contrast to  $\text{LaMnO}_3$ , we found some stable solutions with different orbital orderings in  $\text{KCuF}_3$ . In Fig. 5, we present the total energy of the paramagnetic phase (obtained by averaging the total energies of eight magnetic configurations) for each of the orbital ordered states obtained against the number of paramagnetic iterations. The corresponding angular

distributions of the  $e_g$  electron-spin density for every solution (at the 120th iteration) are shown (bottom row of orbital structures in Fig. 5). As seen from Fig. 5, the ferro-orbitally ordered state (F) has the highest total energy. For this case, the same  $d_{x^2-y^2}$  orbitals at all Mn sites (set as the starting orbital polarization, upper row of Fig. 5) changes to almost fully occupied  $d_{3z^2-r^2}$  orbitals during the paramagnetic iterations (bottom row in Fig. 5). More preferable in energy are two (almost degenerate) solutions which correspond to G- and C-type orbital ordering. Their  $\phi_1$  and  $\phi_2$  orbitals that diagonalize the  $e_g$  occupation matrix are  $d_{x^2-z^2}$  and  $d_{y^2-z^2}$ , staggering in the  $ab$  plane, but having ferro- or antiferro-orbital alignments along the  $c$  axis for C or G-type ordering, respectively. This result agrees with previous theoretical and experimental studies on orbital structures in  $\text{KCuF}_3$ <sup>2,21,15</sup>.

The fourth calculation, which was started from A-type antiferro-orbital ordering, had an oscillating total energy curve up to about the 50th paramagnetic iteration, then seemed to be stabilized with the lowest total energy and with almost fully occupied  $d_{3z^2-r^2}$  orbitals at all Mn sites (the orbital polarization picture at the 60th paramagnetic iteration was found to be close to the F-ordered configuration (see the bottom row of orbital structures in Fig. 5), but with an alternation of few occupied  $d_{x^2-z^2}$  and  $d_{y^2-z^2}$  orbitals along the  $c$  direction). Further paramagnetic iterations resulted in a sharp increase of the total energy of this A-type solution, and at the 120th iteration the orbital structure is an alternation of  $d_{3z^2-r^2}$  and  $d_{3x^2-r^2}/d_{3y^2-r^2}$  orbitals. Thus, from the behaviour of the total energy curves of these four solutions we conclude that paramagnetic  $\text{KCuF}_3$  with uniform  $\text{CuF}_6$  octahedra possesses two orbital orderings which are energy degenerate.

In summary, in this work we presented the new ASS calculation scheme to treat a paramagnetic state. Using this scheme, we successfully described the experimental magnetic/orbital phase diagram of  $\text{LaMnO}_3$ . The orbital ordering in the paramagnetic perovskite manganite is the same type as in the antiferromagnetic phase. A small decrease of the order parameter of the orbital ordering under the AFM-PM transition is in agreement with the observed one. We demonstrated that orbital ordering in both  $\text{LaMnO}_3$  and  $\text{KCuF}_3$  is of purely electronic origin .

Work was supported by the Russian Foundation for Basic Research (grant RFFI-01-02-17063) and the U.S. Department of Energy (grant No. DE-F602-88ER45372).

## REFERENCES

<sup>1</sup> J. B. Goodenough, Phys. Rev. **100**, 564 (1955).

<sup>2</sup> K. I. Kugel and D. I. Khomskii, Sov. Phys. Usp. **25**, 231 (1982).

<sup>3</sup> A. M. Oleś, M. Cuoco and N. B. Perkins, (unpublished) cond-mat/0012013

<sup>4</sup> E. O. Wollan and W. C. Koehler, Phys. Rev. **100**, 545 (1955).

<sup>5</sup> K. Terakura, J. Lee, J. Yu, I. V. Solovyev and H. Sawada, Mater. Sci. Engineering **B63**, 11 (1999).

<sup>6</sup> Y. Murakami, J. P. Hill, D. Gibbs, M. Blume, I. Koyama, M. Tanaka, H. Kawata, T. Arima, Y. Tokura, K. Hirota and Y. Endoh, Phys. Rev. Lett. **81**, 582 (1998).

<sup>7</sup> Tapan Chatterji, G.J. McIntyre, W. Caliebe, R. Suryanarayanan, G. Dhalenne and A. Revcolevschi, Phys. Rev. B **61**, 570 (2000).

<sup>8</sup> K. I. Kugel and D. I. Khomskii, Zh. Eksp. Teor. Fiz. (Sov. Phys. JETP) **64** (37), 1429 (1973).

<sup>9</sup> T. Hotta, S. Yunoki, M. Mayr and E. Dagotto, Phys. Rev. **60**, R15009 (1999).

<sup>10</sup> L. F. Feiner and A. M. Oleś, Phys. Rev. **59**, 3295 (1999).

<sup>11</sup> J. Rodriguez-Carvajal, M. Hennion, F. Moussa, A. H. Moudden, L. Pinsard and A. Revcolevschi, Phys. Rev. B **57**, R3189 (1998).

<sup>12</sup> Q. Huang, A. Santoro, J. W. Lynn, R. W. Erwin, J. A. Borchers, J. L. Peng and R. L. Greene, Phys. Rev. B **55**, 14987 (1997).

<sup>13</sup> M. T. Hutchings, E. J. Samuelson, G. Shirane and K. Hirakawa, Phys. Rev. **188**, 919 (1969).

<sup>14</sup> A. Okazaki, J. Phys. Soc. Jpn. **26**, 870 (1969); **27**, 518 (1969).

<sup>15</sup> A. I. Lichtenstein, J. Zaanen and V. I. Anisimov, Phys. Rev. B **52**, R5467 (1995).

<sup>16</sup> V. I. Anisimov, J. Zaanen and O. K. Andersen, Phys. Rev. B **44**, 943 (1991); V. I. Anisimov, F. Aryasetiawan and A. I. Lichtenstein, J.Phys.:Condens. Matter **9**, 767 (1997).

<sup>17</sup> S. Satpathy, Z. S. Popovic and F. R. Vukajlovic, Phys. Rev. Lett. **76**, 960 (1996).

<sup>18</sup> I. Solovyev, N. Hamada and K. Terakura, Phys. Rev. B **53**, 7158 (1996).

<sup>19</sup> A. Vegas *et. al*, Acta Crystallogr., Sect. B: Struct. Sci. **42**, 167 (1986).

<sup>20</sup> J. F. Mitchell, D. N. Argyriou, C. D. Potter, D. G. Hinks, J. D. Jorgensen and S. D. Bader Phys. Rev. B. **54**, 6172 (1996).

<sup>21</sup> K. Hirakawa and Y. Kurogi, Progr. Theor. Phys. (Suppl.) **46**, 147 (1970).

## FIGURES

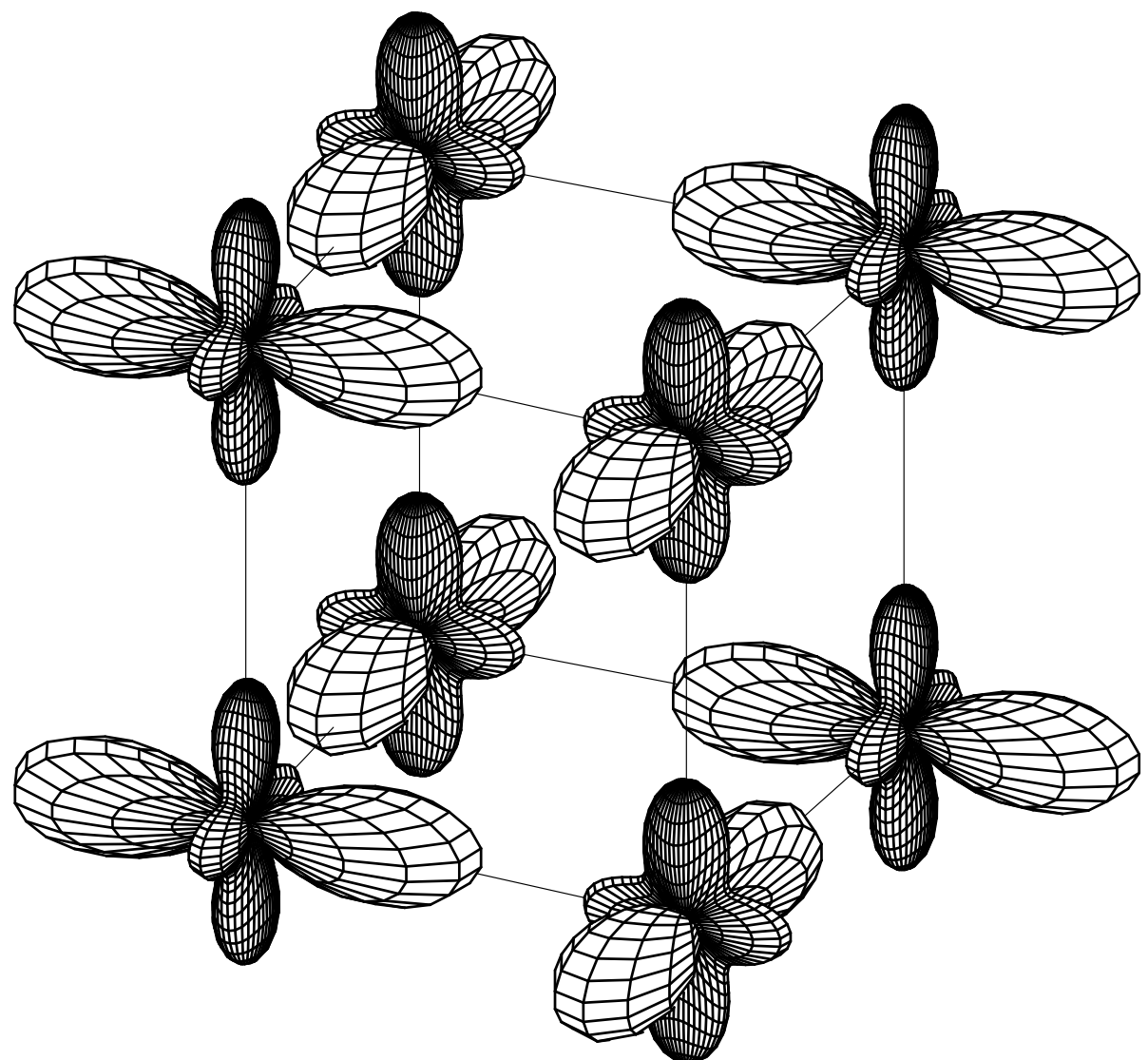
FIG. 1. The calculated angular distribution of the  $e_g$ -electron spin density in the A-type antiferromagnetic phase of  $\text{LaMnO}_3$  from the LDA+U calculations.

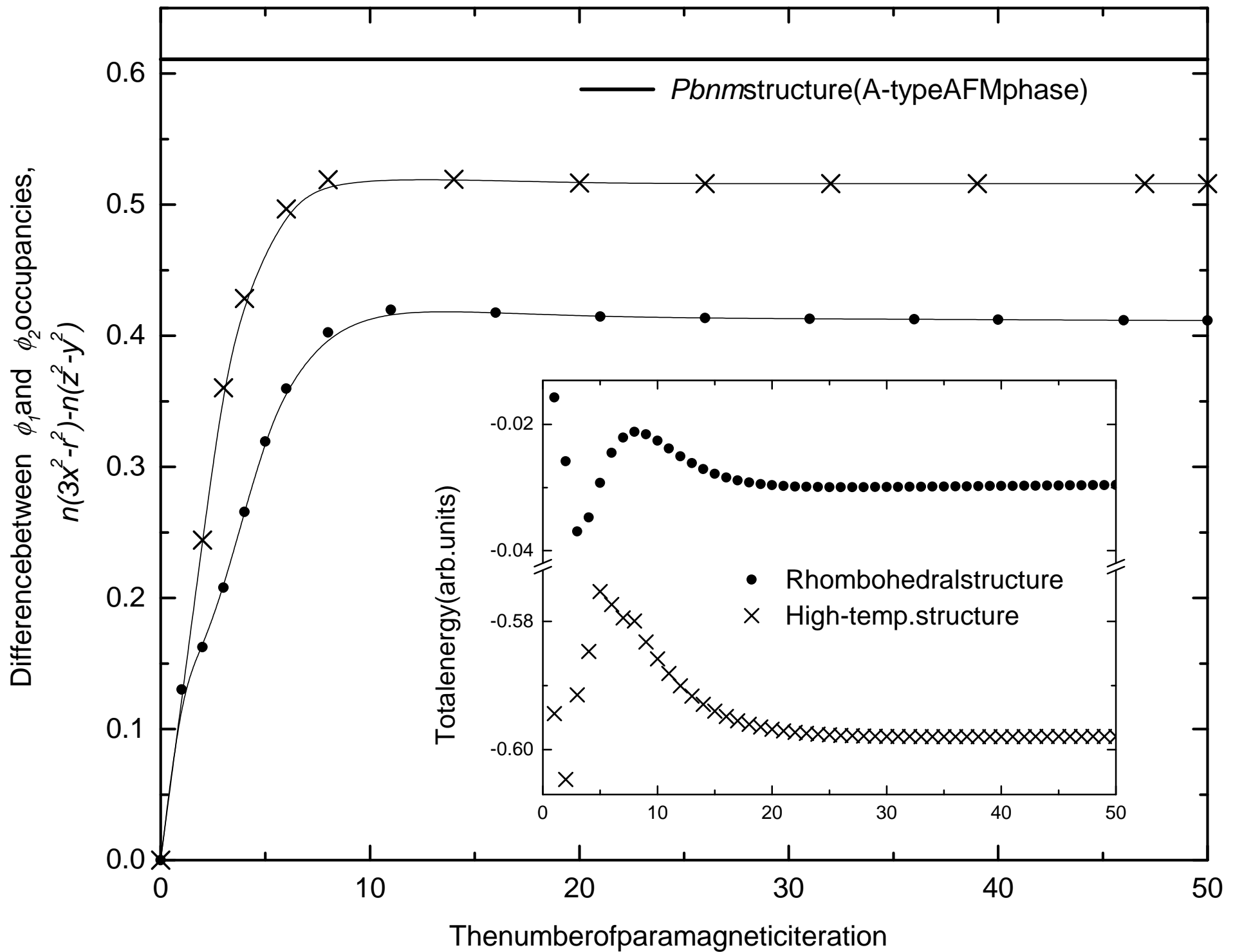
FIG. 2. Dependence of the occupancy difference on the number of paramagnetic iterations for the high-temperature paramagnetic phase,  $\delta_{JT}=0.023$  (crosses) and rhombohedral paramagnetic phase,  $\delta_{JT}=0.000$  (circles) of  $\text{LaMnO}_3$ . The horizontal line stands for calculated orbital order of  $Pbm_n$  A-type AFM phase  $\delta_{JT}=0.133$ . In the insert, the total energy averaged over all magnetic configurations is giving as a function of the number of paramagnetic iteration for the two paramagnetic phases.

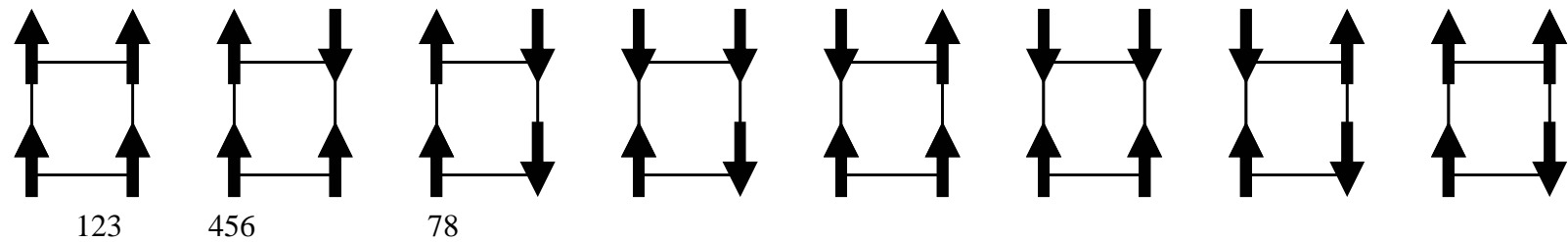
FIG. 3. (a) Schematic illustration of all possible spin configurations in the unit cell which contains four formula units (4 magnetic atoms). Only the  $ac$  plane is shown.

(b) Deviations of the difference between  $\phi_1$  and  $\phi_2$  occupancies in each of the spin configurations considered from the averaged value as a result of ASS calculations of the high-temperature PM phase of  $\text{LaMnO}_3$ . Only the first (broken line) and fiftieth (solid line) iterations are shown.

FIG. 4. Total energies of four solutions with different orbital orderings for  $\text{KCuF}_3$  as a function of the number of paramagnetic iterations. The corresponding orbital structures (F-type ferro-orbital and A-, C- or G-type antiferro-orbital orderings) are shown for the begining (top row) and the 120th iteration (bottom row).







(a)

Difference between  $\phi_1$  and  $\phi_2$  occupancies,  
 $n(3x^2-r^2)-n(z^2-y^2)$

